

Sub-Task 3.4S

Advances in the Science of Laser-Induced Incandescence

Gregory J. Smallwood

ICPET, National Research Council Canada
Ottawa, Ontario, Canada

There have been major advances in the understanding of the physics and chemistry related to the nano-scale processes that occur as a result of the rapid heating and cooling of soot nanoparticles due to laser irradiation. The processes attracting the most attention are the heat and mass transfer processes that govern energy transfer in laser-induced incandescence. A recent workshop series on the science of LII has been established, with the first meeting held in Duisburg, Germany in September, 2005, and the second in Bad Herrenalb in August, 2006. This workshop series will continue on a two-year cycle, occurring just before each International Combustion Symposium, with the next workshop scheduled for July 31 – August 1, 2008, in Ottawa, Canada. Three key themes have evolved from the workshops, namely theory and modeling, experimental procedure, and signal evaluation for LII. The international LII community has established a web presence for the sharing of information about the science of LII, with results from the recent workshops, a forum, and a comprehensive bibliography of literature. The website is located at <http://liiscience.org>.

There are four contributions to report under this sub-task that address the three theme areas identified above:

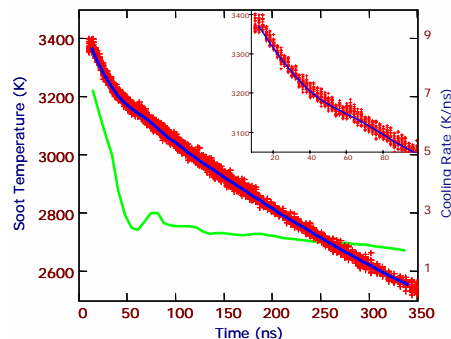
Analysis of Prompt Heat Transfer to Interpret Anomalies Observed with Two-Colour Laser-Induced Incandescence (2C-LII)

Gregory J. Smallwood, David R. Snelling, Fengshan Liu, and Kyle J. Daun
ICPET, National Research Council Canada, Ottawa, Ontario, Canada

Concern has been raised over the observed rapid initial decay of temperature during and immediately after the laser pulse in laser-induced incandescence. This impedes the ability to make meaningful interpretation of signal and/or temperature decays for the sizing of soot nanoparticles. This anomalous behaviour is also shown to affect low-fluence measurements of soot volume fraction in low ambient temperature environments. It is proposed and evidence provided that the reason for this behaviour is that $E(m)$ from the unperturbed soot at the lower measurement wavelength is high, possibly due to absorbed large PAH's or graphitization of the soot. At high fluence the initial cooling rate is shown to be much lower than that predicted by sublimation models.

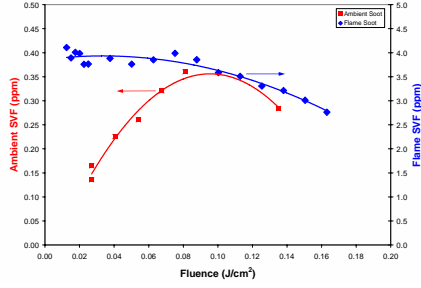
Introduction

The decay of temperature immediately after the peak of the laser pulse has been frequently observed to exhibit an accelerated rate for a short period of time (<100ns). Furthermore, numerous anomalies with LII have been observed, and these anomalies are substantially more evident when applying low-fluence LII to examine post-flame soot at lower ambient temperatures than when in-flame soot is studied. These anomalies include the soot volume fraction (SVF) varying with fluence, the absorption $E(m)$ needed to predict the peak temperature appearing to vary with fluence, and the LII signal intensity required to produce a given temperature varying with fluence.



Evidence

For soot at flame temperatures, the apparent SVF is essentially constant with fluence until the sublimation threshold is reached, after which it decreases with increasing laser fluence. However,

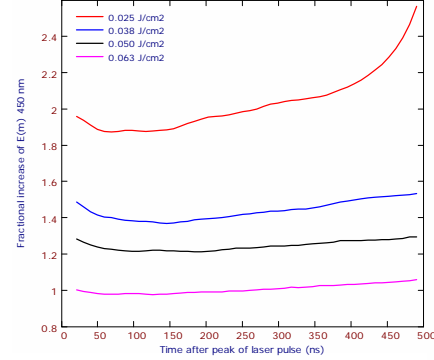


for soot initially at ambient temperatures, as the fluence is increased there is a large increase in apparent SVF until it reaches a maximum at the sublimation threshold, after which SVF decreases.

Analysis

Assuming there is no real variation of SVF with fluence then at a single experimental condition the observed LII temperature can be used to “calibrate” the intensity, producing a scale factor to be applied to the Boltzmann equation to give the observed intensity. At the lowest fluence the intensity determined temperature is much lower than the LII temperature, with the higher wavelength based temperature being lower than that calculated from the intensity at the lower wavelength, but this discrepancy decreases as the fluence is increased.

The proposed explanation for this behaviour is that $E(m)$ from the unperturbed soot at the lower wavelength is high, possibly due to absorbed large PAH's or graphitization of the soot, and that the laser heating causes a surface modification, “cleaning” the surface.



Assuming the SVF and $E(m)$ at the higher wavelength are constant, the intensity based temperatures can be used to deduce the required increase in $E(m)$ to result in the three temperatures coinciding.

Changes in the soot emissivity in the 350-500 nm range would explain the low fluence anomalies.

Heat Conduction from Spherical Nano-particles

F. Liu, K. J. Daun, G. J. Smallwood, and D. R. Snelling
National Research Council of Canada, Ottawa, Canada, K1A 0R6

This study describes the physics of conduction heat transfer from nano-sized spherical particles and interpolation techniques used to calculate heat transfer in the transition regime. The accuracy of these techniques is evaluated by comparing their results with those obtained by direct Monte Carlo simulation.

Introduction

An accurate model of conduction heat transfer from a small sphere immersed in a gas and an understanding of the underlying physics are essential when analyzing data from time-resolved laser-induced incandescence experiments. This work summarizes recent reviews [1, 2] of this problem.

The governing physics is specified by the Knudsen number, $Kn = \lambda_{MFP}/a$. If Kn is very large, heat transfer occurs in the free-molecular regime. In this regime molecules travel between the particle and the equilibrium gas without colliding, and the heat transfer rate is given by

$$q_{FMR}(Kn) = \alpha_T \pi a^2 \frac{P_g \bar{c} \gamma^* + 1}{2 \gamma^* - 1} \left(\frac{T_p}{T_g} - 1 \right), \quad (1)$$

where α_T is the thermal accommodation coefficient, \bar{c} is a characteristic molecular speed, and γ^* is the temperature-averaged adiabatic gas

constant. The heat transfer rate increases with increasing molecular number density and is thus proportional to P_g and Kn^{-1} .

If Kn is very small heat transfer occurs in the continuum regime,

$$q_c = 4 \pi a \bar{k}_c (T_p - T_g), \quad (2)$$

where \bar{k}_c is the temperature-averaged thermal conductivity. In this regime q_c is independent of pressure and Kn since increasing P_g increases the molecular number density but decreases the distance between intermolecular collisions.

If Kn is neither small nor large conduction occurs in the transition regime. The physics of this regime is dominated by a collisionless layer surrounding the particle that causes a temperature jump at the gas-surface interface. Since the Boltzmann equation is analytically intractable in this regime, heat transfer is estimated using schemes that interpolate between q_{FMR} and q_c .

Transition-Regime Interpolation Schemes

Transition-regime interpolation schemes are either simple-interpolative, diffusion-approximation, or boundary-sphere methods. The most popular simple-interpolative technique is by McCoy and Cha [3], who define an overall collision frequency as the sum of intermolecular and molecule-wall collision frequencies. Substituting this into the Chapman-Enskog approximation for q_c results in

$$\frac{q_{\text{trans}}(\text{Kn})}{q_c} = \frac{1}{1 + G \text{Kn}}, \quad (3)$$

where G is a geometry-specific parameter.

Diffusion-approximation (DA) techniques estimate q_{trans} using Eq. (2) but adjust T_p to account for the temperature-jump as specified by the slip parameter ξ . After rearranging, it can be shown that

$$\frac{q_{\text{trans}}(\text{Kn})}{q_c} = \frac{1}{1 + \xi \text{Kn}}, \quad (4)$$

where ξ is given by Loyalka [4].

Boundary-sphere (BS) methods work by finding the unknown temperature at the interface of the collisionless layer and the continuum gas, T_δ , by solving $q_{\text{FMR}}(T_p, T_\delta) = q_c(T_\delta, T_g)$. Although this is traditionally done analytically, a numerical technique [2] has recently been proposed that accounts for temperature-dependent gas properties.

Figure 1 shows solutions obtained using the interpolation schemes and by direct Monte Carlo simulation. Note that temperature-dependent gas properties must be considered when analyzing LII data, and the Loyalka DA model only applies to monatomic gases. The BS method of [2] is the most accurate scheme for analyzing LII data.

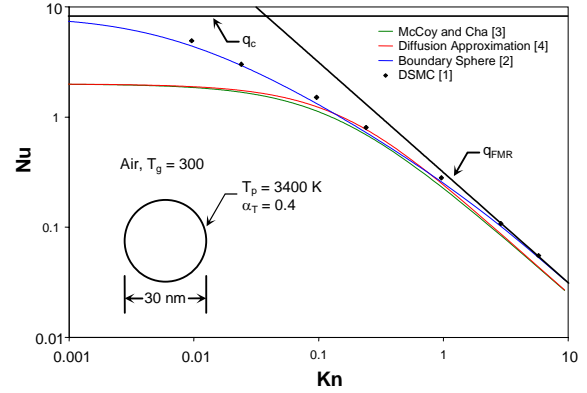


Fig. 1: Transition-Regime Interpolation Schemes and DSMC Results

References

- [1] F. Liu, K. J. Daun, D. R. Snelling, G. J. Smallwood, *App. Phys. B*, 83, 3, 355-382 (2006).
- [2] A. V. Filippov, D. E. Rosner, *IJHMT* 43 127-138 (2000).
- [3] B. J. McCoy, C. Y. Cha, *Chem. Eng. Sci.* 29, 381-388 (1974).
- [4] S. K. Loyalka, *Prog. Nuc. Energy* 12, 1-56 (1983).

Measuring Accommodation Coefficients using Laser-Induced Incandescence

K. J. Daun, G. J. Smallwood, F. Liu, and D. R. Snelling
National Research Council of Canada, Ottawa, Canada, K1A 0R6

This study presents thermal accommodation coefficients between soot and different gases. The dependence of these values on the molecular mass of the gas is investigated.

Introduction

Laser-induced incandescence has recently been used to measure thermal accommodation coefficients, α_T . Although most experiments carried out to date provide soot/air or soot/flame-gas accommodation coefficients, a recent study [1] presents α_T values between soot and four other gases. The present study expands this data to include more gases and explores the relationship between α_T and the molecular mass of the gas.

Theory

Although the physics of gas-surface interactions is highly complex and not fully understood, several phenomenological models accurately describe the dependence of α_T on different parameters, the most important being the ratio of the molecular mass of the gas and the atomic mass of the surface atoms, $\mu = m_g/m_a$. The earliest and most robust model was proposed by Baule [2, 3], who predicted α_T based on the kinetic energy transferred when a moving rigid sphere representing a gas molecule collides with

a stationary rigid sphere representing a surface atom,

$$\alpha_T = \frac{2.4 \mu}{(1 + \mu)^2}. \quad (1)$$

This model is physical only if $\mu < 1$, since the surface atom could not otherwise back-scatter the gas molecule. If $\mu > 1$, lattice forces between multiple surface atoms help repel incident gas molecules. Burke and Hollenback [4] suggest that m_a can be adjusted to account for these forces.

Experimental Apparatus

Soot is extracted at a height of 52 mm above a Gülder burner operating at conditions described in [5], and is induced into a motive gas in the venturi section of a mini-eductor resulting in dilution ratios between 30:1 and 100:1. The mixture flows into a closed chamber where two-color laser-induced incandescence is carried out. The thermal accommodation coefficient is then calculated from the effective temperature time-decay following the procedure described in [5].

Results

Values of α_T between soot and different gases are plotted in Fig. 1. The accommodation coefficient increases with increasing m_g for monatomic gases as predicted by Baule theory, but decreases for diatomic gases.

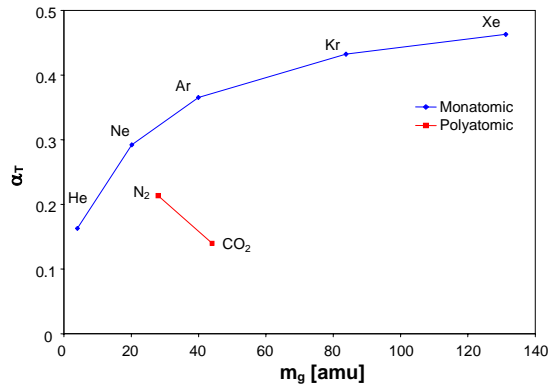


Fig. 1: Experimentally-determined values of α_T between soot and different gases

Figure 2 shows the monatomic gas data plotted with Eq. (1) assuming an effective atomic surface mass of 119 amu, determined by a least-squares fit. Although the general trend of the data agrees with the Baule model, Eq. (1) is not a good fit to the data if m_s is constant. A better fit is found by letting m_s be a function of m_a , which is consistent with the theory proposed in [3]. Values of m_s were solved by fitting Eq. (1) to the experimentally-measured α_T values for monatomic gases, and were found to be a hyperbolic function of m_a , as shown in Fig. 2.

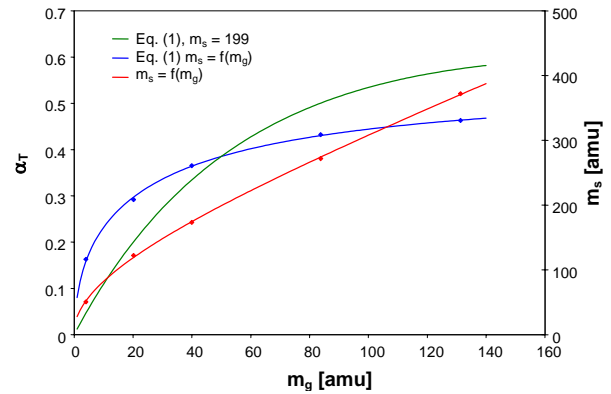


Fig. 2: Comparison of Baule theory to experimentally-determined α_T values for monatomic gases.

References

- [1] A. V. Eremin, E. V. Gurentsov, M. Hofmann, B. F. Kock, C. Schulz, *App. Phys. B*, 83, 449-454 (2006).
- [2] B. Baule, *Ann. Physik*, 44, 145-176 (1914).
- [3] F. O. Goodman, *Surf. Sci.*, 3, 386-414 (1965).
- [4] J. R. Burke, D. J., Hollenbach, *Astrophysical J.* 265, 223-234 (1983).
- [5] D. R. Snelling, F. Liu, G. J. Smallwood, Ö. L. Gülder, *Comb. and Flame*, 136 180-190 (2004)

Design Optimization for High Sensitivity Two-Color LII

Gregory J. Smallwood, David R. Snelling, Robert A. Sawchuk, Dan Clavel, and Daniel Gareau
ICPET, National Research Council Canada, Ottawa, Ontario, Canada

The development of a high sensitivity LII (HS-LII) experimental apparatus is discussed. The target was to improve the sensitivity of an auto-compensating laser induced incandescence (AC-LII) system employing two-wavelength pyrometry and low-fluence excitation by two orders of magnitude. The design considerations and implementation through a number of iterations of improvement are discussed. All aspects of the system were considered for optimization. The principle of the *Lagrangian invariant* was found to be

most effective in designing the optical receiver subsystem. Application of the HS-LII instrument to measurements of soot concentration in the ambient atmosphere is presented, demonstrating a 500-fold improvement.

Introduction

The IPCC National Greenhouse Gas Inventories Programme is now focusing on emission estimation of aerosols relevant to climate change, and there is a need to measure black carbon levels in the atmosphere at microgram per cubic metre or lower mass concentrations. At the same time, emission standards for Diesel particulate matter (PM) are being lowered dramatically, resulting in the adoption of Diesel particulate filters (DPFs) by manufacturers, and there is a need to measure solid carbon levels in the exhaust and in dilution tunnels at microgram per cubic metre or lower mass concentrations.

Development of high sensitivity LII to measure soot concentration at ambient levels for monitoring emissions from post-2007 Diesel engines, urban air quality, black carbon in atmosphere, and emissions from aircraft at altitude is required. The target for the high sensitivity LII system is a measurement limit of 0.05 ppt ($\sim 0.1 \mu\text{g}/\text{m}^3$) or less.

Methodology

The current limit for measuring soot concentration with the NRC Mobile II AC-LII system is about 5 ppt (nearly $10 \mu\text{g}/\text{m}^3$). The new design therefore requires a 100-fold improvement in sensitivity. Additionally, it is desirable to retain the low fluence and two-color pyrometry features of auto-compensating laser induced incandescence (AC-LII), and to make the system portable/mobile.

The approach was to optimize all aspects of the laser-induced incandescence method, including the laser, beam generation optics, sampling cell, receiver collection optics, receiver filters and dichroics, photodetectors, signal detection and digitization electronics, and the signal analysis software.

The *Lagrangian invariant* principle was applied to constrain the design of collection optics and receiver, as preservation of the Lagrangian invariant is essential for a lossless optical system. The concept is that the minimum product of the numeric aperture and aperture diameter

cannot be improved upon, $L = NA1 \cdot R1 = NA2 \cdot R2 = \text{constant}$

for optimum design. The probe volume diameter was based on the maximum practical Lagrangian invariant of receiver optical system, and the probe volume depth was set by desired laser fluence and maximum available laser energy. Optimization recommended that the crossing angle be minimized, but it was constrained by practicality.



Optical layout of first generation high sensitivity system HS-LII-1

Results

A comparison of the calibration constants for a number of AC-LII systems shows that the target of a 100-fold improvement in sensitivity has been far exceeded.

System	λ_1 (nm)	RCS ($\text{W}/\text{m}^2 \cdot \text{sr} \cdot \text{Volt}$)	Increase relative to Mobile II	λ_2 (nm)	RCS ($\text{W}/\text{m}^2 \cdot \text{sr} \cdot \text{Volt}$)	Increase relative to Mobile II
Mobile II	397	$2.54 \cdot 10^{10}$	–	782	$4.22 \cdot 10^{10}$	–
HS-LII-1	445	$9.43 \cdot 10^5$	26,900x	746	$4.41 \cdot 10^6$	95.7x
HS-LII-2	445	$9.14 \cdot 10^5$	27,800x	753	$1.36 \cdot 10^7$	3100x
Artium LII-200	402	$4.39 \cdot 10^8$	57.9x	782	$4.62 \cdot 10^9$	9.13x
Artium ES-LII-200	447	$2.20 \cdot 10^8$	115x	829	$1.91 \cdot 10^9$	22.1x

Recent measurements of ambient air in Ottawa have demonstrated the ability to measure concentrations below 0.010 ppt ($< 20 \text{ ng}/\text{m}^3$), 500 times lower than previously measured.

